Metal-metal transition in perovskite $PbRuO_3$

J.-G. Cheng, J.-S. Zhou,* and J. B. Goodenough
Texas Materials Institute, University of Texas at Austin, Austin, Texas 78712, USA
(Received 12 August 2009; revised manuscript received 25 September 2009; published 30 November 2009)

The high-pressure perovskite phase of $PbRuO_3$ is orthorhombic *Pbnm* at room temperature and transforms in a first-order transition to *Imma* below $T_t \approx 90$ K; there is no long-range magnetic order above 1.5 K. We report a systematic study of the transport and magnetic properties versus temperature under high pressure of a single grain as well as the structural study under high pressure at room temperature. We found a metal-metal transition at 90 K in contrast to the semiconductor-insulator transition reported in the literature. We also compare the LT *Imma* phase of $PbRuO_3$ with the *Imma* phase found in the $Sr_{1-x}Ba_xRuO_3$ system. An important hybridization of the Pb-6*s* and Ru-4*d* orbitals is implicated.

DOI: 10.1103/PhysRevB.80.174426 PACS number(s): 71.30.+h, 75.30.Et

Ferromagnetism with a maximum Curie temperature $T_c \sim 164$ K in the metallic perovskite ruthenates has not been well understood. The saturation moment 1.4–1.6 μ_B at 5 K in $SrRuO_3$ is slightly below the spin-only value of a localized electron model for this t^4 electron system, but it is significantly larger than that expected from a model of very weak itinerant-electron ferromagnetism. The Curie temperature shows an interesting evolution as Ca^{2+} or Ba^{2+} is substituted for Sr^{2+} and the maximum T_c is found at $SrRuO_3$.[1–4] Unlike the rare-earth R^{3+} substitution in perovskite $R^{3+}M^{3+}O_3$ systems, the steric effect on T_c in the $A^{2+}Ru^{4+}O_3$ family cannot be extracted from T_c versus the *A*-site ionic radius since the substitution introduces a significant change of chemistry as well as the size variance. Chemical substitution suppresses the Curie temperature for both Ba and Ca substitution, but the metallic phase remains to the lowest temperature over the entire $ARuO_3$ family. Since the ionic radius of Pb^{2+} is between those of Sr^{2+} and Ba^{2+}, a steric-effect consideration would predict that the perovskite $PbRuO_3$ is a ferromagnetic metal. It would be surprising if the high-pressure phase of $PbRuO_3$ has a semiconductor behavior near room temperature and transfers into an insulator phase through a first-order transition at 90 K and shows no magnetic order down to 1.5 K as recently reported by Kimber *et al.*[5] Their observation highlighted a possible $6s^2$ "lone pair" effect and a hybridization between Pb-6*s* and Ru-4*d* electrons that could change the electronic state in $PbRuO_3$ dramatically.

The perovskite $PbRuO_3$ was first synthesized under 9 GPa and 1400 °C in the 1960s.[6] However, its low-temperature crystal structure and properties were not characterized. Kimber *et al.* have shown that $PbRuO_3$ undergoes a structural transition from the *Pbnm* phase to the *Imma* phase on cooling through a first-order transition at about 90 K. The local structural distortions resolved from a neutron diffraction study suggested an orbital ordering on Ru(IV) in the low-temperature *Imma* phase. Moreover, a first-principles calculation in the same report justified the insulator ground state of the *Imma* phase. All the experimental results and the self-consistent justification of an insulator ground state reported by Kimber *et al.*[5] appear to be flawless except for one observation; a temperature-dependent paramagnetic susceptibility shows the presence of a magnetic moment on at least some of the Ru(IV) ions, so it becomes necessary to justify why a magnetic-insulator phase, especially with orbital ordering, does not result in spin ordering. Kimber *et al.* suggested that the bending of the Ru-O-Ru bond angle from 180° weakens the superexchange interaction. However, the 159.8° Ru-O-Ru bond angle they reported is too large to suppress magnetic interactions between localized spins; provided that the M-O-M bond angle falls into the range 142° to 156° in 3*d* transition-metal oxides with orthorhombic perovskite structure, most of them exhibit spin-ordering transitions. This inconsistency motivated us to reexamine the transport and magnetic properties of the $PbRuO_3$ perovskite phase and to study the peculiar *Imma* phase under high pressure. Instead of an insulator at low temperatures, our transport studies reveal a metal-metal transition at 90 K. The Pb-6*s* and Ru-4*d* orbital hybridization appears to broaden the bandwidth so as to suppress magnetic ordering.

Our perovskite $PbRuO_3$ samples were synthesized in a Walker-type multianvil module (Rockland Research). As originally reported,[6] we have found that the perovskite phase can be stabilized under a pressure $P > 9$ GPa and temperature $T > 1300$ °C. The x-ray powder diffraction (XRD) and its profile fitting through the Rietveld refinement show in Fig. 1 that our samples have precisely the same crystal structure as that reported by Kimber *et al.* The XRD at low temperatures on our sample also revealed a phase transition to the *Imma* phase at about 80 K. The oxygen stoichiometry is another factor to consider. Kimber *et al.* have verified their sample is close to stoichiometry within 1% by the site occupation from refining their neutron-diffraction data. From electron energy loss spectroscopy (EELS), we have obtained the ratio $O/Ru = 3 \pm 1$ from sampling points on scanning across a crystal grain (most points fall on the line of 3). All these comparisons indicate that samples from the two groups are identical. In order to explain the discrepancy of the transport properties found between our samples and that by Kimber *et al.*, we provide here a detailed description of our procedure of sample characterization and measurements. The synthesis at $T \approx 1400$ °C and $P > 9$ GPa always gives perovskite samples with large grains; the longest dimension is about 200 μm as seen from scanning electron microscopy (SEM). These grains are loosely connected and can be separated easily by a pair of tweezers. Cracks were developed during cooling of these high-pressure products, which results in a noisy signal and many sharp up-and-down changes in $\rho(T)$ if the measurement was made directly on pellets from

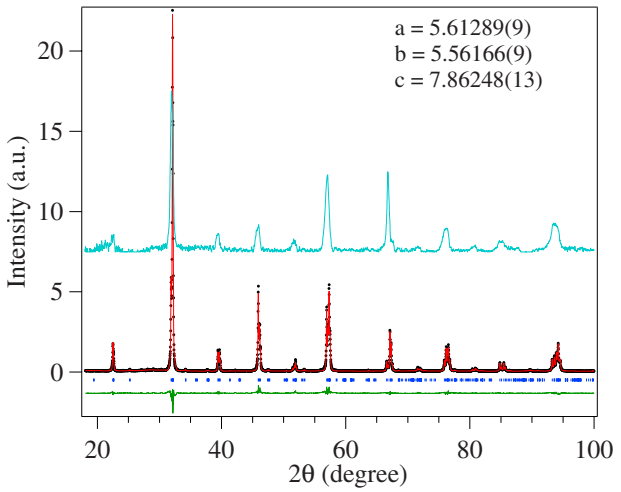

FIG. 1. (Color online) X-ray powder diffraction (Cu-kα) and its profile fitting by Rietveld refinement of the orthorhombic $PbRuO_3$. The XRD in middle is obtained from integrating the diffraction pattern of Fig. 2.

high-pressure synthesis. We have chosen to make measurements on single grains separated from the high-pressure products. Selected grains were mounted on a thin glass fiber and then placed in a four-circle diffractometer (Bruker P4) for a rotation-sample x-ray diffraction (RSXRD). Diffractions were collected by an image plate from Fuji. The x-ray beam size is about 500 μm and grains were located in the center of the beam, which insures that we have checked the entire part of the grain. Spots in the RSXRD picture of Fig. 2 confirm that the grain included large domains. The possible twining and the multidomain character of the selected grains prevented structural determination by single-crystal diffraction. However, as superimposed in Fig. 1, the intensity versus 2θ integrated from the RSXRD patterns by using the software *fit2d* confirms that the structure is the same as that from the XRD of a bulk sample and no impurity phase was found. All measurements of transport properties were made on small single-crystal grains that had been checked by RSXRD. Four Cu leads (12 μm dia.) were attached on a grain with silver epoxy and cured at 150 °C for 20 min. The contact resistance is a couple of ohms. Due to the small sample size, a pair of differential thermal couples were attached to two copper leads from a grain; the distance between contact points and the grain is about 100 μm. Therefore, the temperature gradient measured is slightly larger than that actually applied on the grain; as a result, the magnitude of the thermoelectric power shown is slightly smaller than that we obtained on a polycrystalline pellet by a regular method. However, results from these two methods have the same temperature dependence. Measurements under pressure were made in Be-Cu high-pressure cells; the cell for magnetization measurement fits a commercial superconducting quantum interference device (SQUID) magnetometer from Quantum Design. The samples were placed inside a Teflon cell filled with a 1:1 mixture of 3M Fluorinert FC77 and FC72 as the pressure medium. In the magnetic-susceptibility measurement, a small piece of Pb was used as the pressure manometer whereas the pressure was monitored by a

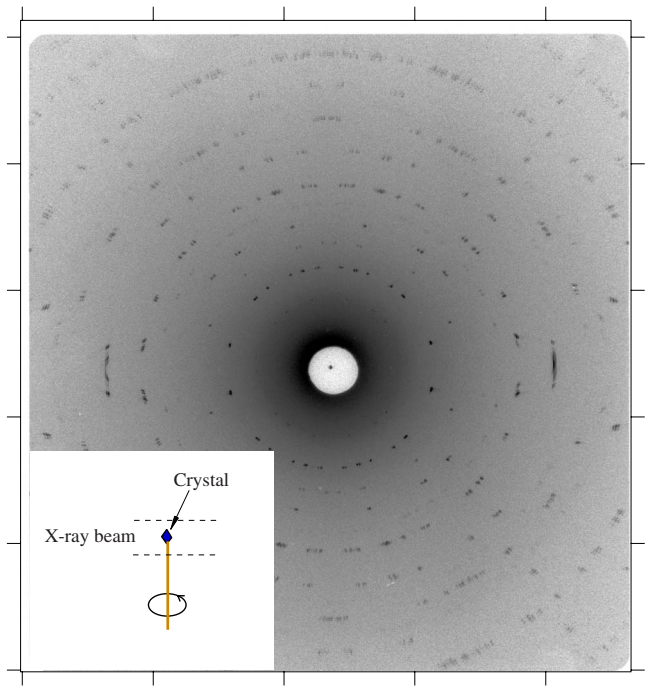

FIG. 2. (Color online) The rotation sample x-ray diffraction. The inset illustrates the configuration how the diffraction was performed.

manganin-wire coil in the measurements of transport properties. The same configuration for the RSXRD was also used to study the crystal structure of $PbRuO_3$ under pressure. In this case, a diamond anvil cell was placed in the position of the sample in the P4 diffractometer. A small amount of CaF_2 powder as pressure manometer was mixed with the sample, and a mixture of methanol and ethanol 4:1 was used as the pressure medium.

The temperature-dependent magnetic susceptibility of Fig. 3(a) is nearly identical to that reported by Kimber *et al.*; on cooling, $\chi(T)$ exhibits an abrupt drop at T_t=89 K followed by a broad maximum near 25 K. A curve fitting to the formula $\chi(T)=\chi_0+C/(T+\theta)$ in the temperature range $T>T_t$ suggests that the *Pbnm* phase might have become antiferromagnetic below a $T_N<T_t$. Since no classic spin ordering was detected down to 1.5 K,[5] the broad hump in $\chi(T)$ signals AF spin fluctuations at $T<25$ K. As shown in Fig. 3(b), the structural transition, which is monitored by an anomaly of $\chi(T)$ at T_t, is dramatically suppressed under pressure since pressure prefers the *Pbnm* phase, which has a smaller cell volume than the *Imma* phase at low temperatures. In sharp contrast to what was observed by Kimber *et al.*, our sample exhibits metallic conductivity down to 5 K in Fig. 4. Corresponding to the structural transition at T_t, $R(T)$ shows a distinct anomaly that has a very small hysteresis loop between the cooling and warming measurements. The $R(T)$ at ambient pressure was reproduced after releasing pressure. Similar to the pressure dependence of T_t from the magnetic susceptibility $\chi(T)$ in the inset of Fig. 3, T_t is reduced under pressure. Both the hysteresis loop and the anomaly in $R(T)$ at T_t become smaller under higher pressure.

The thermoelectric power measurements of Fig. 5 provide

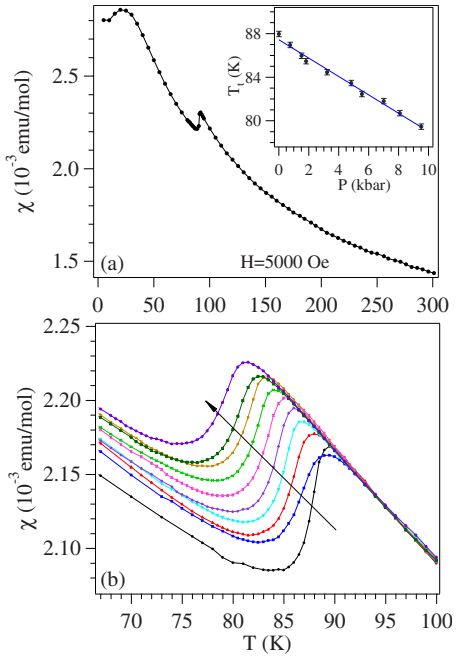

FIG. 3. (Color online) (a) Temperature dependence of magnetic susceptibility of the perovskite $PbRuO_3$; (b) A zoom-in plot of (a) near the structural transition temperature T_t under pressure. The arrow points to the direction of increasing pressure; inset: pressure dependence of the transition temperature T_t.

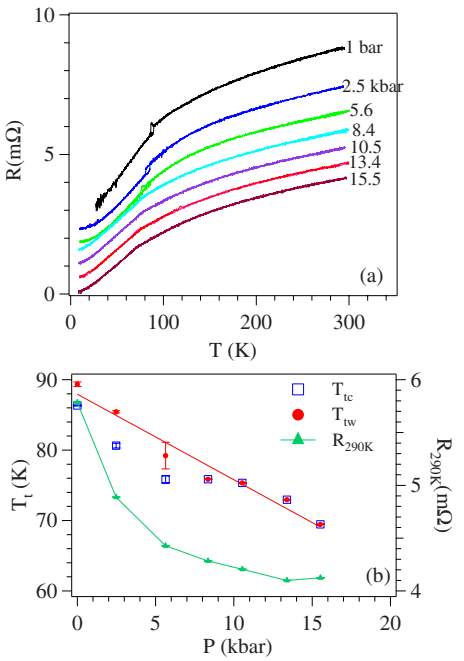

FIG. 4. (Color online) (a) Temperature dependence of resistance of the perovskite $PbRuO_3$ under pressure; curves have been shifted vertically for clarification; (b) Pressure dependence of T_t obtained from (a) during the cooling down and warming up and the resistance at 290 K.

more information about the low-temperature (LT) *Imma* phase and the high-temperature (HT) *Pbnm* phase. $S(T)$ in the HT phase is typical for a metal,[7] i.e., it follows the Mott diffusive thermoelectric power formula at sufficiently high temperature and shows the phonon drag effect at low temperature. Although $S(T)$ of the HT phase is truncated by the phase transition at T_t, it approaches zero near 100 K, which indicates that the phonon-drag effect contributes a negative correction $\Delta S(T)$ to $S(T)$. The phase transition at T_t brings about an abrupt change of S to a more negative value. The $S(T)$ of the LT phase seems to have a large contribution from the phonon-drag effect. The phonon-drag effect is much more enhanced in broad-band metals like Cu, Au, Pt[8]; it was barely seen in the narrow-band metal $LaCuO_3$ and is completely suppressed in Nd doped $La_{1-x}Nd_xCuO_3$.[9] The relationship between the bandwidth and the phonon-drag effect has been further demonstrated by the $S(T)$ measurements of $La_{1-x}Nd_xCuO_3$ under high pressure.[9] The strong phonon-drag effect found in the LT phase of high-pressure $PbRuO_3$ signals that it is a broad-band metal. As shown in Fig. 5(a), whereas pressure changes slightly the $S(T)$ in the *Pbnm* phase, it enhances significantly the phonon-drag effect in the LT *Imma* phase. Whether the correction to $S(T)$ from the phonon-drag effect is positive or negative depends on the nature of the electron-phonon interactions that produce it; normal electron-phonon interactions contribute a negative correction whereas Umklapp processes give a positive one.[6] Whereas the $S(T)$ of the HT phase is reproducible for different samples, the strong phonon-drag effect in the LT phase, which is negative for the grain used in our high-pressure measurement, was found to be positive in some other samples, i.e., the $S(T)$ showed a mirror symmetry around the $S=0$ line of the $S(T)$ in Fig. 5(a). It means that the sign of the correction from the phonon-drag effect is determined by the residual strain built into the high-pressure products. Given the same contact resistance, the noise level of $S(T)$ is much reduced in the LT phase from that in the HT phase, which could also serve as an indicator for a more conductive LT phase. High pressure does not cause any permanent change on the sample since the original $S(T)$ under ambient pressure is fully recovered after releasing pressure.

As seen from $S(T)$ at ambient pressure in Fig. 5, a sharp transition at T_t becomes broader for $P>10$ kbar, but T_t could still be defined by a shoulder of $S(T)$. The pressure dependence of T_t defined in this way is nearly the same as that from $\chi(T)$ and $R(T)$. However, as demonstrated in Fig. 5(b), another sharp transition develops at $T_t'<T_t$ under $P \geq 8$ kbar. Although the resistance measurement $R(T)$ and the thermoelectric measurement $S(T)$ were made on the same grain, no anomaly has been found at T_t' in $R(T)$. A large hysteresis loop in $S(T)$ at T_t' indicates it is another first-order transition. Thermoelectric power is related to the asymmetric factor of a dispersion curve at the Fermi energy; it is more sensitive than the conductivity measurement to a phase transition in most cases. It remains unknown whether the transition at T_t' corresponds to a change in the magnetic susceptibility measurement since the maximum pressure of the cell for $\chi(T)$ measurement is below 1 GPa. The LT *Imma* phase is confined to an extremely narrow range near the end member $PbRuO_3$ in the phase diagram of the $Pb_{1-x}Sr_xRuO_3$ system.[10] However, the high-pressure phase below T_t' has been found in $Pb_{0.9}Sr_{0.1}RuO_3$ where no LT *Imma* phase is found under ambient pressure. The structural study at low

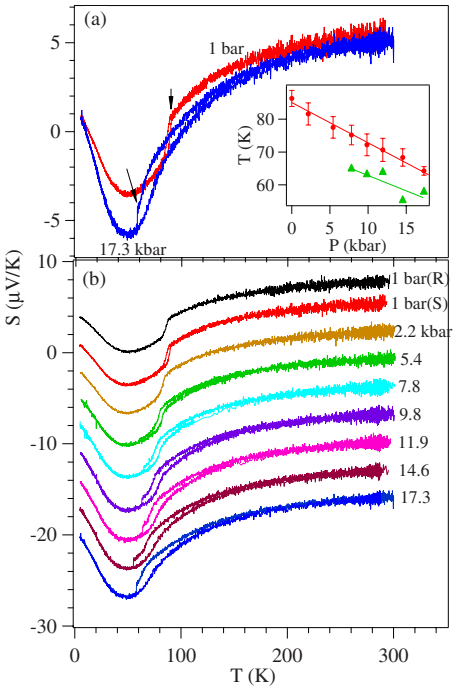

FIG. 5. (Color online) Temperature dependence of thermoelectric power of the perovskite $PbRuO_3$. (a) S(t) at ambient pressure and the highest pressure in this study; the plot is to highlight the absolute change induced by high pressure. The arrow near the curve at 1 bar points to the phase transition at T_t, which develops into a shoulder-like transition under high pressure. The arrow near the curve at 17.3 kbar points to a sharp transition at T_t'. Inset: the pressure dependences of transition temperatures T_t and T_t'. (b) $S(t)$ curves for all pressures. Curves have been shifted vertically for clarification.

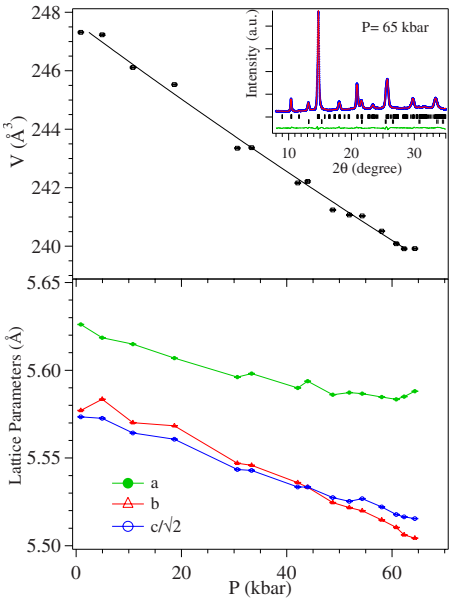

FIG. 6. (Color online) Pressure dependences of lattice parameters of the perovskite $PbRuO_3$. Error bars are smaller than symbols. Lattice parameters were obtained from the profile fitting of XRD. An example of XRD (wavelength $\lambda=0.71069$ Å) under high pressure and the profile fitting are shown as inset which includes diffractions from both the perovskite $PbRuO_3$ and CaF_2 to monitor the pressure.

temperatures and under high pressure with synchrotron radiation is in progress in order to identify the new high-pressure phase below T_t' in $Pb_{1-x}Sr_xRuO_3$. Results from these future study have no overlap with the fact of a metal-metal transition at T_t in $PbRuO_3$ established in this work.

It is highly unusual to find that the *Imma* phase with higher symmetry than the *Pbnm* phase occurs at low temperatures. One may wonder what is the difference between this *Imma* phase and that found in many perovskite oxides like $Sr_{1-x}Ba_xRuO_3$,[10] $Sr_{1-x}A_xSnO_3$ (A=Ca, Sr, and Ba),[11] $SrZrO_3$,[12] and $SrRuO_3$ (Ref. 13) where the geometric tolerance factor t is increased by either substituting a larger ion in the A site as in the first two systems or by raising temperature as in the latter two systems. In the tilting systems of the perovskite structure,[14] *Pbnm* is a subgroup of *Imma*. A series of structural transitions in the order of $Pbnm \rightarrow Imma \rightarrow I4/mcm(R3\text{-}c$ in some cases$) \rightarrow Pm\text{-}3m$ has been found as the t factor increases. As a precursor for the phase transition from *Pbnm* to *Imma*, a crossover from $b>a$ to $a>b$ and a continuous increase of $a-b$ are always found in the *Pbnm* phase near the *Pbnm-Imma* boundary. It has been shown that an increased octahedral-site distortion with O-M-O bond angle $\alpha<90°$, where α subtends the axis of cooperative octahedral-site rotation, is the origin of the lattice-parameter crossover.[15] The structural transitions from *Pbnm* to *Imma* and to $I4/mcm$ before the final cubic phase relieve this local distortion. Therefore, the maximum $a-b$ is found at the phase boundary between *Pbnm* and *Imma*. Since *Pbnm* is a subgroup of *Imma*, i.e., one tilting component of the *Pbnm* structure vanishes continuously at the phase boundary, the transition from *Pbnm* to *Imma* has been found to be second order. The first-order transition at T_t indicates that the *Imma* phase found in $PbRuO_3$ at low temperatures is not induced by the tolerance factor as occurs with the *Imma* phase that we have normally seen in the chain of phase transitions of perovskite structure. Moreover, an abrupt increase in $a-b$ has been found in the LT *Imma* phase at T_t whereas it should change continuously in a phase transition from the *Pbnm* phase to the normal *Imma* phase.

Figure 6 shows room-temperature lattice parameters of the perovskite $PbRuO_3$ under pressure. The *Pbnm* phase is stable to 65 kbar, the highest pressure in this study. The bulk modulus obtained by fitting the V versus P curve with the Birch-Murnaghan equation is 185(4) GPa, which is in line with that of other perovskite ruthenates, 192 GPa in $SrRuO_3$ (Ref. 16) and 182 GPa in $BaRuO_3$ (Ref. 17) provided that the ion size of Pb^{2+} is located between those of Sr^{2+} and Ba^{2+}. The bulk modulus has been found generally to be proportional to the inverse of the cell volume in the perovskite oxides.[18] The lattice-parameter difference $a-b$ increases continuously with increasing pressure, which indicates that pressure increases the octahedral-site distortion by reducing further the angle α. This pressure-induced structural change would normally lead eventually to a phase transition to the *Imma* phase. In contrast, as shown by the physical properties under pressure, pressure reduces T_t, which implies that pressure suppresses the LT *Imma* phase in the perovskite $PbRuO_3$.

After highlighting the differences between the LT *Imma* phase of $PbRuO_3$ and the *Imma* phase normally found at high temperatures and high pressure, we take a closer look at the LT phase. Structural data from Kimber *et al.* show that one of the O_1-Ru-O_2 angles, which is 91.35° in the Pbnm phase, increases abruptly to 91.71° in the LT *Imma* phase. As a result, this bond-angle change brings five Pb-O bonds falling to 2.5 Å. In comparison, there are only three Pb-O bonds with bond length less than 2.5 Å at 300 K. The coordination change appears to enhance the pathway for the hybridization between Pb-6*s* and Ru-4*d* orbitals so as to broaden the bandwidth of the Ru-O array. To increase the hybridization is likely the driving force for the first-order transition at T_t at the expense of the cell volume. High pressure prefers the *Imma* phase normally seen at high temperature but suppresses the LT *Imma* phase in the $PbRuO_3$. The bond-length splitting at the octahedral site of Ru(IV) below T_t found by Kimber *et al.* is not a solid proof of an orbital ordering since a similar bond length splitting has been found in $SrRuO_3$ at 100 K.[19]

In conclusion, the low-temperature phase with *Imma* space group found in the perovskite $PbRuO_3$ is different from the *Imma* phase in other perovskite oxides such as $Sr_{1-x}Ba_xRuO_3$. High pressure favors the *Imma* phase in the second-order *Pbnm* to *Imma* phase transition in perovskites, but it suppresses the low-temperature *Imma* phase in the perovskite $PbRuO_3$. Our results of transport properties show that the phase transition from *Pbnm* to *Imma* phase at $T_t \approx 90$K is a metal-metal transition. As supported by the structural data, an enhanced hybridization of the Pb-6s and Ru-4d orbitals below T_t broadens the π^* conduction band of Ru(IV):*t* (Ref. 4) parentage on the RuO_3 array. Our thermoelectric power data also suggest a broader bandwidth in the LT *Imma* phase. The suppression of a ferromagnetic transition in the perovskite phase of $PbRuO_3$ is likely due to a bandwidth broadening as in the case of cubic $BaRuO_3$ under 8 GPa.[20]

ACKNOWLEDGMENT

We thank the Robert A. Welch Foundation (Grant No. F-1066) and NSF (Grant No. DMR0904282) for financial support. J.S.Z. thanks H. D. Zhou for the XRD measurement at low temperatures.

*jszhou@mail.utexas.edu

[1] J. M. Longo, P. M. Raccah, and J. B. Goodenough, J. Appl. Phys. **39**, 1327 (1968).
[2] G. Cao, S. McCall, M. Shepard, J. E. Crow, and R. P. Guertin, Phys. Rev. B **56**, 321 (1997).
[3] K. Yoshimura, T. Imai, T. Kiyama, K. R. Thurber, A. W. Hunt, and K. Kosuge, Phys. Rev. Lett. **83**, 4397 (1999).
[4] C.-Q. Jin, J.-S. Zhou, J. B. Goodenough, Q. Q. Liu, J. G. Zhao, L. X. Yang, Y. Yu, R. C. Yu, T. Katsura, A. Shatskiy, and E. Ito, Proc. Natl. Acad. Sci. U.S.A. **105**, 7115 (2008).
[5] S. A. J. Kimber, J. A. Rodgers, H. Wu, C. A. Murray, D. N. Argyriou, A. N. Fitch, D. I. Khomskii, and J. P. Attfield, Phys. Rev. Lett. **102**, 046409 (2009).
[6] J. A. Kafalas and J. M. Longo, Mater. Res. Bull. **5**, 193 (1970).
[7] S. J. Blatt, P. A. Schroeder, C. L. Foiles, and D. Grieg, *Thermoelectric Power of Metals* (Plenum, New York, 1976).
[8] D. K. C. MacDonald, *Thermoelectricity: An Introduction to the Principles* (Wiley, New York, 1962).
[9] J.-S. Zhou, W. Archibald, and J. B. Goodenough, Phys. Rev. B **57**, R2017 (1998).
[10] J.-G. Cheng, J.-S. Zhou, and J. B. Goodenough (unpublished).
[11] E. H. Mountstevens, J. P. Attfield, and S. Redfern, J. Phys.: Condens. Matter **15**, 8315 (2003).
[12] C. J. Howard, K. S. Knight, B. J. Kennedy, and E. H. Kisi, J. Phys.: Condens. Matter **12**, L677 (2000).
[13] B. J. Kennedy, B. A. Hunter, and J. R. Hester, Phys. Rev. B **65**, 224103 (2002).
[14] R. H. Mitchell, *Perovskites, Modern and Ancient*, (Almaz Press Inc., Ontario, 2002).
[15] J.-S. Zhou and J. B. Goodenough, Phys. Rev. Lett. **94**, 065501 (2005).
[16] M. K. Jacobsen, R. S. Kumar, G. Cao, J. J. Neumeier, and A. L. Cornelius, J. Phys. Chem. Solids **69**, 2237 (2008).
[17] J.-S. Zhou (unpublished).
[18] N. L. Ross and R. J. Angel, Am. Mineral. **84**, 277 (1999).
[19] G. Leitus, S. Reich, and F. Frolow, J. Magn. Magn. Mater. **206**, 27 (1999).
[20] J.-S. Zhou, K. Matsubayashi, Y. Uwatoko, C.-Q. Jin, J.-G. Cheng, J. B. Goodenough, Q. Q. Liu, T. Katsura, A. Shatskiy, and E. Ito, Phys. Rev. Lett. **101**, 077206 (2008).